Cancer Cell
Article

Modulation of K-Ras-Dependent Lung Tumorigenesis by MicroRNA-21

Mark E. Hatley,[1,2] David M. Patrick,[2] Matthew R. Garcia,[1] James A. Richardson,[2,3] Rhonda Bassel-Duby,[2] Eva van Rooij,[2,4] and Eric N. Olson[2,*]
[1]Department of Pediatrics
[2]Department of Molecular Biology
[3]Department of Pathology
University of Texas Southwestern Medical Center, Dallas, TX 75390-9148, USA
[4]Present address: miRagen Therapeutics, Boulder, CO 80301-3695, USA
*Correspondence: eric.olson@utsouthwestern.edu
DOI 10.1016/j.ccr.2010.08.013

SUMMARY

Lung cancer is the leading cause of cancer-related deaths in the world, and non-small-cell lung cancer (NSCLC) accounts for 80% of cases. *MicroRNA-21* (*miR-21*) expression is increased and predicts poor survival in NSCLC. Although miR-21 function has been studied in vitro with cancer cell lines, the role of miR-21 in tumor development in vivo is unknown. We utilize transgenic mice with loss-of-function and gain-of-function *miR-21* alleles combined with a model of NSCLC to determine the role of miR-21 in lung cancer. We show that overexpression of *miR-21* enhances tumorigenesis and that genetic deletion of *miR-21* partially protects against tumor formation. MiR-21 drives tumorigenesis through inhibition of negative regulators of the Ras/MEK/ERK pathway and inhibition of apoptosis.

INTRODUCTION

MicroRNAs are evolutionarily conserved, endogenous, non-protein-coding, ~20–23 nucleotide single-stranded RNAs that negatively regulate gene expression in a sequence-specific manner (Cho, 2007; Esquela-Kerscher and Slack, 2006; Voorhoeve and Agami, 2007). The human genome is predicted to encode as many as 1000 miRNAs, or ~3% of the total number of human genes (Bartel, 2004; Esquela-Kerscher and Slack, 2006). The 5′ portion of miRNA sequence containing bases two to eight, termed the "seed" region, is important in target mRNA recognition. miRNAs negatively regulate target gene expression through complementarity between the miRNA seed sequence and the target mRNA 3′ untranslated region (UTR). miRNAs that bind with perfect complementarity to the protein encoding messenger RNA (mRNA) target the mRNA for destruction, whereas miRNAs with imperfect complementarity to the 3′ UTR of the mRNA target repress mRNA translation. Expression of approximately 30% of human proteins appears to be regulated by miRNAs (Lewis et al., 2005). Through interactions with 3′ UTRs, miRNAs can modulate the expression of many genes simultaneously, often regulating individual signaling pathways at multiple levels (Baek et al., 2008; Selbach et al., 2008).

An integral role of miRNAs in cancer pathogenesis has begun to emerge. miRNA expression profiling reveals characteristic signatures for many tumor types, including non-small-cell lung cancer (NSCLC) (Volinia et al., 2006), and are predictive of tumor classification, prognosis, and response to therapy (Calin and Croce, 2006). miRNA expression patterns are remarkably reliable markers of cancers; in some cases, they have even proven more reliable than conventional histology (Subramanian et al., 2008). MicroRNAs are capable of functioning as classical tumor suppressors or oncogenes, thus actively participating

Significance

MicroRNAs are small noncoding RNAs that are commonly dysregulated in human malignancies and play a substantial role in the pathogenesis and survival of many cancers. MiR-21 is overexpressed in the majority of human malignancies, including non-small-cell lung cancer (NSCLC). However, it is not clear whether miR-21 determines important aspects of lung cancer pathogenesis or is instead simply a marker for advanced disease. We show in vivo that miR-21 expression increases with oncogenic K-ras activation and modulates NSCLC tumorigenesis by targeting *Spry1*, *Spry2*, *Btg2*, and *Pdcd4*, which act as negative regulators of the Ras/MEK/ERK pathway, and *Apaf1*, *Faslg*, *Pdcd4*, and *RhoB*, which promote apoptosis. *MiR-21* deletion also sensitizes cells to DNA-damaging chemotherapy, suggesting that miR-21 inhibition could be of therapeutic value.

in human cancer pathogenesis (Ventura and Jacks, 2009). Recently, gain- and loss-of-function studies in mice demonstrate critical roles for miR-26a and miR-9 in hepatocellular carcinoma and breast cancer metastasis, respectively (Kota et al., 2009; Ma et al., 2010). These data suggest that the pattern of miRNA expression contributes to fundamental aspects of tumor biology.

A large-scale survey to determine the miRNA signature of 540 tumor samples—including lung, breast, stomach, prostate, colon, and pancreatic tumors and their respective normal adjacent tissue—revealed miR-21 was the only miRNA upregulated in all these tumors (Volinia et al., 2006). Further miRNA profiling in tumor samples and cancer cell lines showed increased miR-21 expression in glioblastoma (Chan et al., 2005; Ciafre et al., 2005), head and neck carcinomas (Tran et al., 2007), ovarian cancer (Iorio et al., 2007), B cell lymphoma (Lawrie et al., 2007), hepatocellular (Meng et al., 2007), and cervical carcinoma (Lui et al., 2007). These studies clearly illustrate miR-21 dysregulation in tumors; however, the studies do not prove a causal role for miR-21 in cancer pathogenesis.

Functional studies in cancer cell lines suggest that miR-21 has oncogenic activity. Knockdown of miR-21 in cultured glioblastoma cells activates caspases leading to apoptotic cell death, suggesting miR-21 is an antiapoptotic factor (Chan et al., 2005). In breast cancer MCF-7 cells, miR-21 knockdown results in suppression of cell growth in vitro and tumor growth in xenografts (Si et al., 2007). Knockdown of miR-21 in the metastatic breast cancer MD-MBA-231 cells reduced invasion and metastasis (Zhu et al., 2008). Targeted deletion of *miR-21* in RKO and DLD1 colon cancer cells revealed that *miR-21* contributes to tumorigenesis through compromising cell cycle progression and DNA damage-induced checkpoint function through the *CDC25A* target gene (Wang et al., 2009). These studies indicate knockdown of miR-21 expression in cancer cell lines results in phenotypes important for tumor biology. However, the potential role of miR-21 in tumorigenesis in vivo has not yet been explored.

Lung cancer is the most common form of cancer in the world, accounting for approximately 12.3% of all cancers with an estimated 1.2 million new cases each year (Parkin et al., 2001). Lung cancer is also the leading cause of cancer-related deaths in the world, with NSCLC accounting for 80% of all cases (Ramalingam et al., 1998). Despite novel therapies and advances in early detection, NSCLC is often diagnosed at an advanced stage and has a poor prognosis, with a median survival of 8 to 11 months and a 5 year survival rate in patients with NSCLC of only 13% using conventional cytotoxic chemotherapy (Soon et al., 2009). Recently, miR-21 expression levels have proven useful prognostic markers in NSCLC (Markou et al., 2008; Yanaihara et al., 2006). The level of miR-21 expression in sputum distinguishes patients with NSCLC from cancer-free control subjects with a greater sensitivity than conventional cytology (Xie et al., 2010). Currently, more experiments are needed to determine whether miR-21 participates in driving the malignant phenotype or simply reflects the cellular stress.

In the current study, we used transgenic mice with both loss-of-function and gain-of-function *miR-21* alleles in combination with the K-ras^{LA2} mouse model of NSCLC to elucidate the role of miR-21 in NSCLC pathogenesis.

RESULTS

miR-21 Overexpression Promotes Tumor Development In Vivo

Increased expression of miR-21 in human cancer could reflect malignant physiology or could determine important aspects of cancer biology. To address this question, we generated transgenic mice that overexpress the *miR-21* gene and mice with deletion of the *miR-21* gene and tested the consequences in a mouse model of NSCLC. We designed a strategy to conditionally overexpress miR-21 using the Cre-lox system and the CAG-Z-EGFP vector (see Figure S1A and Supplemental Experimental Procedures available online) (Fukuda et al., 2005). Global miR-21 overexpression was achieved by breeding the *CAG-Z-miR21-EGFP* mouse to transgenic mice expressing Cre recombinase from the ubiquitous CAG promoter resulting in the *CAG-miR-21* mouse, which globally overexpressed miR-21 4- to 6-fold over normal levels of expression (Figures S1B–S1D). *CAG-miR-21* transgenic mice were viable, fertile, and born in expected Mendelian ratios. miR-21 expression increases in mouse models of cardiac hypertrophy and following myocardial infarction; however, adult male *CAG-miR-21* mice showed no signs of heart failure compared to littermate controls (Figure S1E) (van Rooij et al., 2006; van Rooij et al., 2008).

To explore the role of miR-21 in the pathogenesis of NSCLC, we utilized the K-ras^{LA2} murine lung cancer model, which harbors a targeted, latent *K-ras G12D* allele that is activated by two distinct recombination events (Johnson et al., 2001). The first occurs in ES cells, and the second occurs in vivo, resulting in the random activation of the mutant *K-ras G12D* allele in somatic cells. K-ras^{LA2} mice develop multifocal lung tumors with 100% penetrance, and less frequently develop thymic lymphomas and skin papillomas (Johnson et al., 2001). *CAG-miR-21; K-ras^{LA2}* compound mutant mice were generated by breeding to compare the number, rate of formation, and histology of tumors relative to littermate control *K-ras^{LA2}* mice. Remarkably, overexpression of *miR-21* enhanced the number of tumors in this model of lung cancer (Figures 1A–1C). Compared with *K-ras^{LA2}* littermates, *CAG-miR-21;K-ras^{LA2}* mice displayed significantly more lung tumors visible grossly at 18 weeks (Figure 1D) and microscopically on H&E cross-section over all time points (Figure 1F). Total tumor area as a proportion of total lung area was significantly increased with miR-21 overexpression (Figure 1E).

Tumors in *CAG-miR-21;K-ras^{LA2}* mice exhibited increased proliferation compared with *K-ras^{LA2}* control tumors (Figure 1G). Despite the increased tumor burden, the survival of *CAG-miR-21;K-ras^{LA2}* mutant mice did not differ from *K-ras^{LA2}* control mice (Figure 1H). This may be explained by a decreased incidence of thymic tumors in *CAG-miR-21;K-ras^{LA2}* mutant mice compared to *K-ras^{LA2}* controls (Figure 1I), thus contributing to the enhanced survival. Unlike *K-ras^{LA1};p53$^{-/-}$* compound mutant mice (Johnson et al., 2001), we did not observe an increased tumor spectrum or increased metastasis in the *CAG-miR-21;K-ras^{LA2}* mutant mice. miR-21 overexpression increased the incidence of all tumor grades without increasing the rate of conversion to adenocarcinoma, suggesting that miR-21 participates in tumor promotion rather than progression and metastasis in this model (Figures 1J and 1K). miR-21 overexpression

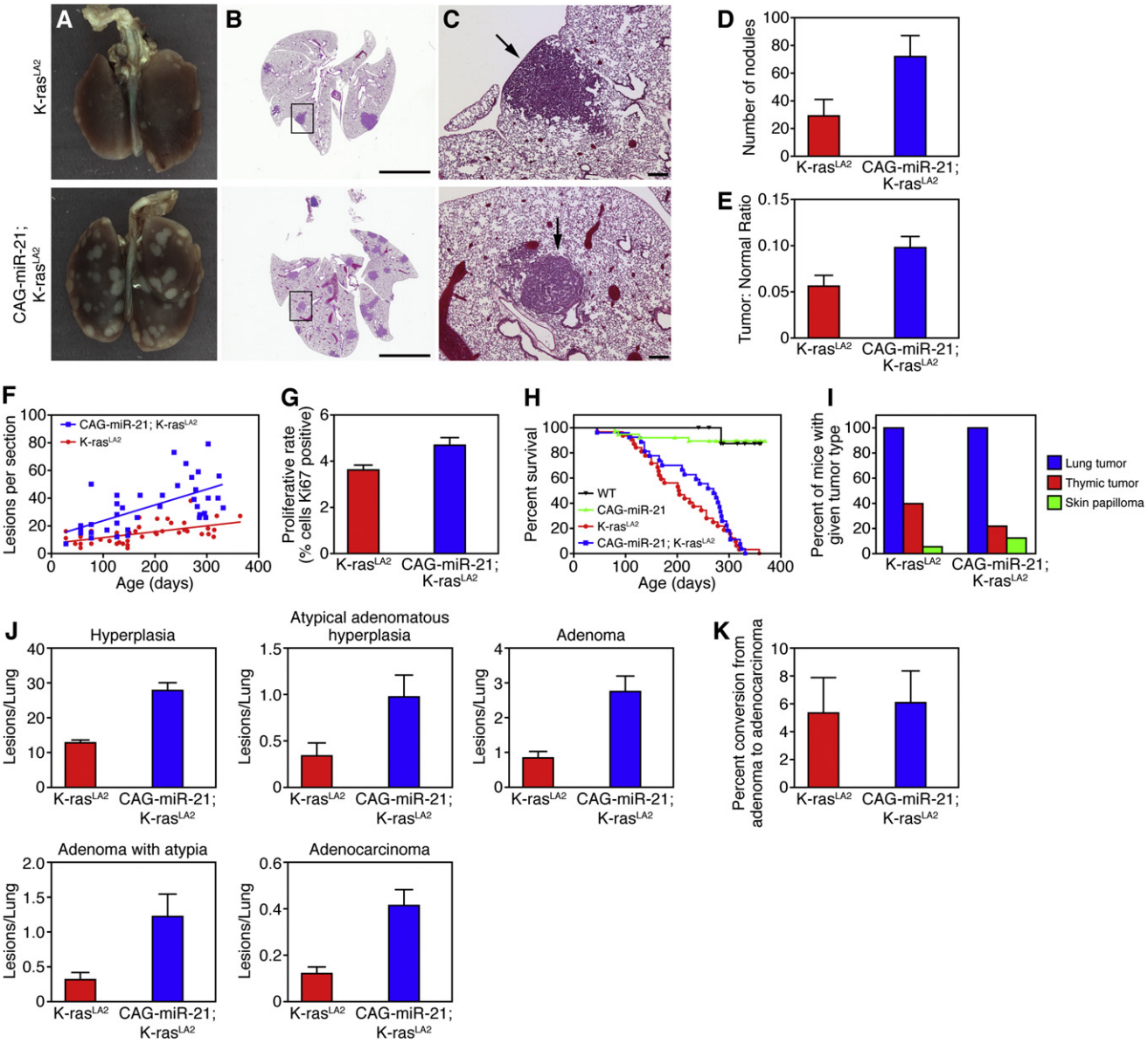

Figure 1. *miR-21* Overexpression Enhances Tumor Formation in the K-ras^{LA2} Mouse Model of NSCLC

(A) Gross (A) and cross-sectional (B and C) H&E histology of lungs isolated from *CAG-miR-21;K-ras^{LA2}* mice and *K-ras^{LA2}* littermate controls at 18 weeks of age. The image in (C) shows magnification of boxed lesions in (B). Arrows in top and bottom panels indicate a hyperplastic lesion and adenoma, respectively. The scale bars represent 5 mm (B) and 200 μm (C).

(D) Nodules grossly visible were counted on the lung surface of *CAG-miR-21;K-ras^{LA2}* (n = 5) and *K-ras^{LA2}* (n = 4) mice sacrificed at 18 weeks of age. Results represent mean ± SEM; p = 0.013 with two-tailed, unpaired Student's t test.

(E) Tumor burden measured as the ratio of total tumor area to total lung area of the lungs counted in (D). Results are mean ± SEM; p = 0.045 using two-tailed, unpaired Student's t test.

(F) Quantification of tumor lesions on lung H&E cross-section from *CAG-miR-21;K-ras^{LA2}* (n = 49) and *K-ras^{LA2}* (n = 40) mice over time. Slopes were determined by linear regression; p = 0.0027.

(G) Quantification of proliferating cells detected by Ki67 antibody immunostaining of lung tumors. Results are mean ± SEM (n = 12); p = 0.01 by two-tailed, unpaired Student's t test.

(H) Survival curve of *CAG-miR-21;K-ras^{LA2}* (n = 27) and *K-ras^{LA2}* (n = 32) mice (p = 0.367) with median survival of 270 and 203 days, respectively; for WT mice, n = 10; for *CAG-miR-21* mice, n = 20.

(I) Tumor spectra in *CAG-miR-21;K-ras^{LA2}* (n = 27) and *K-ras^{LA2}* mice (n = 32).

(J) Lung H&E cross-sections from *CAG-miR-21;K-ras^{LA2}* (n = 27) and *K-ras^{LA2}* (n = 32) mice in the survival cohort were analyzed, and all lesions were classified for tumor grade. For hyperplasia, p < 0.0001. For atypical adenomatous hyperplasia, p = 0.017. For adenoma, p ≤ 0.0001. For adenoma with atypia, p = 0.0042. For adenocarcinoma, p = 0.033. All data are represented as the mean ± SEM of the number of lesions per lung.

(K) Rate of conversion of adenoma to adenocarcinoma. Data are presented as mean ± SEM (p = 0.83). See also Figure S1.

did not increase the rate of recombination of the *K-ras*^{LA2} allele (Figure S1F). We followed *CAG-miR-21* mice (n = 39) without *K-ras*^{LA2} for up to 555 days and performed full necropsy and histological analysis on H&E sections of the following tissues: lung, heart, brain, spleen, liver, kidney, stomach, colon, skeletal muscle, and bone marrow. No tumors were observed in *CAG-miR-21* mice without *K-ras*^{LA2}, indicating that miR-21 overexpression alone is not sufficient for tumorigenesis. These data suggest that *miR-21* overexpression in human tumors does not simply reflect cancer pathology, but instead enhances aspects of the pathology of NSCLC.

miR-21 Deletion Suppresses Ras-Driven Transformation In Vitro

To address the necessity of miR-21 in the development of NSCLC, we generated *miR-21* knockout mice. Homozygous *miR-21* knock-out mice are viable, fertile, and born in expected Mendelian ratios without any gross phenotypic differences compared to wild-type or heterozygous littermates, and without a cardiac phenotype (D.P., E.V.R., and E.N.O., unpublished data). To dissect the role of miR-21 in Ras-driven transformation, we isolated mouse embryonic fibroblasts (MEFs) from wild-type and *miR-21*$^{-/-}$ mice. Northern blot analysis and real-time PCR confirmed deletion of *miR-21* (Figures S2A and S2B). These MEFs were immortalized and transformed with retroviruses expressing SV40 large T and small t antigens and *H-ras*^{G12V}. There was no difference in proliferation between the *miR-21*$^{-/-}$ and wild-type MEFs (Figure S2C). However, the *miR-21*$^{-/-}$ MEFs formed significantly less colonies in soft agar than wild-type MEFs (Figure S2D) and developed smaller tumors in xenografts in nude mice (Figure S2E). These observations suggest that miR-21 actively participates in Ras-driven transformation.

miR-21 Deletion Suppresses Tumor Development In Vivo

Given that high levels of miR-21 expression in patients with NSCLC serve as an independent negative prognostic factor and that miR-21-deficient MEFs form fewer colonies in soft agar, we hypothesized that genetic deletion of *miR-21* in the K-ras^{LA2} model would alter tumorigenesis. To explore this possibility, we crossed the *miR-21*$^{-/-}$ allele into the K-ras^{LA2} NSCLC model. Significantly fewer tumors were present on the surface of the lungs of 20-week-old *miR-21*$^{-/-}$;*K-ras*^{LA2} compound mutant mice compared to *K-ras*^{LA2} control mice (Figures 2A–2C). Total tumor area as a proportion of total lung area was significantly decreased with miR-21 deletion (Figure 2D). *miR-21* deletion did not alter proliferation in tumors measured by Ki67 staining (Figure 2E). *miR21*$^{-/-}$;*K-ras*^{LA2} mice all develop lung tumors, but show an increased incidence of thymic lymphoma (Figure 2F). *miR-21*$^{-/-}$;*K-ras*^{LA2} mutant mice displayed a reduced incidence of hyperplasic lesions and adenomas compared to *K-ras*^{LA2} controls (Figure 2G). Although not statistically significant, there was a trend toward decreased conversion of hyperplasia to adenoma in the *miR-21*$^{-/-}$;*K-ras*^{LA2} mice (Figure 2H). No adenocarcinomas were noted in any of the 14 *miR-21*$^{-/-}$/*K-ras*^{LA2} animals evaluated. These results illustrate that miR-21 deletion suppresses tumor development in vivo.

miR-21 Targets Multiple Tumor Suppressor Genes

To identify miR-21 effectors responsible for phenotypes observed, we utilized two algorithms that predict the mRNA targets of miRNAs, TargetScan (Grimson et al., 2007), and PicTar (Krek et al., 2005). Approximately 180 mRNAs are predicted as miR-21 target genes on the basis of the presence of miR-21 sites in their 3′ UTRs. Many of the miR-21-predicted targets have been reported to function as tumor suppressors and have been validated in vitro in previous studies (Selcuklu et al., 2009). We cloned the 3′ UTRs of 24 putative mouse miR-21 target genes into a luciferase reporter construct. Reporter assays in COS cells revealed miR-21-dependent repression of 13 of the 24 3′ UTRs, and mutation of the miR-21 site in the 3′ UTR abrogated the repression in 11 of the putative target gene 3′ UTRs (Figure 3A). Four of the validated miR-21 target genes are known negative regulators of the Ras/MEK/ERK pathway: sprouty 1 (*Spry1*), sprouty 2 (*Spry2*), B cell translocation gene 2 (*Btg2*), and programmed cell death 4 (*Pdcd4*). Several proapoptotic genes were directly targeted by miR-21, apoptotic peptidase activating factor 1 (*Apaf1*), Fas ligand (*Faslg*), *Pdcd4*, and ras homolog gene family member B (*RhoB*). We show miR-21-dependent repression of the mouse *Apaf1* 3′ UTR reporter; however, the miR-21 site in the human *APAF1* 3′ UTR is conserved in primates but not conserved in the mouse. Eleven of the putative miR-21 target gene 3′ UTRs, including phosphatase and tensin homolog (*Pten*), were not repressed by miR-21 (Figure 3B). Caspase 3 and K-ras do not contain miR-21 sites in their 3′ UTR, and the 3′ UTR luciferase reporter activity is not suppressed by miR-21 (Figure 3B). These results suggest that in vitro miR-21 can repress multiple tumor suppressor genes that may participate in tumorigenesis.

Oncogenic Ras Activation Increases miR-21 Expression In Vivo

Previously, an autoregulatory loop connecting miR-21 and Ras activation through AP-1 was illustrated in a rat thyroid cell system (Talotta et al., 2009). miR-21 expression was induced by AP-1 in response to Ras activation, and *miR-21* mediated Ras-dependent downregulation of *Pdcd4* (Talotta et al., 2009), a known negative regulator of AP-1 transactivation (Goke et al., 2004; Jansen et al., 2005; Yang et al., 2003; Yang et al., 2001). In addition, epidermal growth factor receptor (EGFR) and HER2/*neu* signaling positively regulates miR-21 expression in human lung and breast carcinoma cell lines, respectively (Huang et al., 2009; Seike et al., 2009). We confirmed this autoregulatory loop in vivo by analyzing miR-21 expression in normal lung and tumors of *K-ras*^{LA2} and *CAG-miR-21;K-ras*^{LA2} mutant mice. Normal lung tissue from K-ras^{LA2} mice (prior to K-ras activation) exhibits wild-type expression levels of miR-21 (Figures 4A and 4B). K-ras activation in the tumors of *K-ras*^{LA2} mice increased miR-21 expression by 4-fold, similar to the expression level in the *CAG-miR-21* transgenic mouse lung. In *CAG-miR-21;K-ras*^{LA2} tumors, miR-21 expression was more than additive compared to either *CAG-miR-21* or *K-ras*^{LA2} mice alone. We speculate that, by driving miR-21 expression in the transgenic mouse, we provided a "second hit" prior to K-ras activation, thus accelerating tumor initiation.

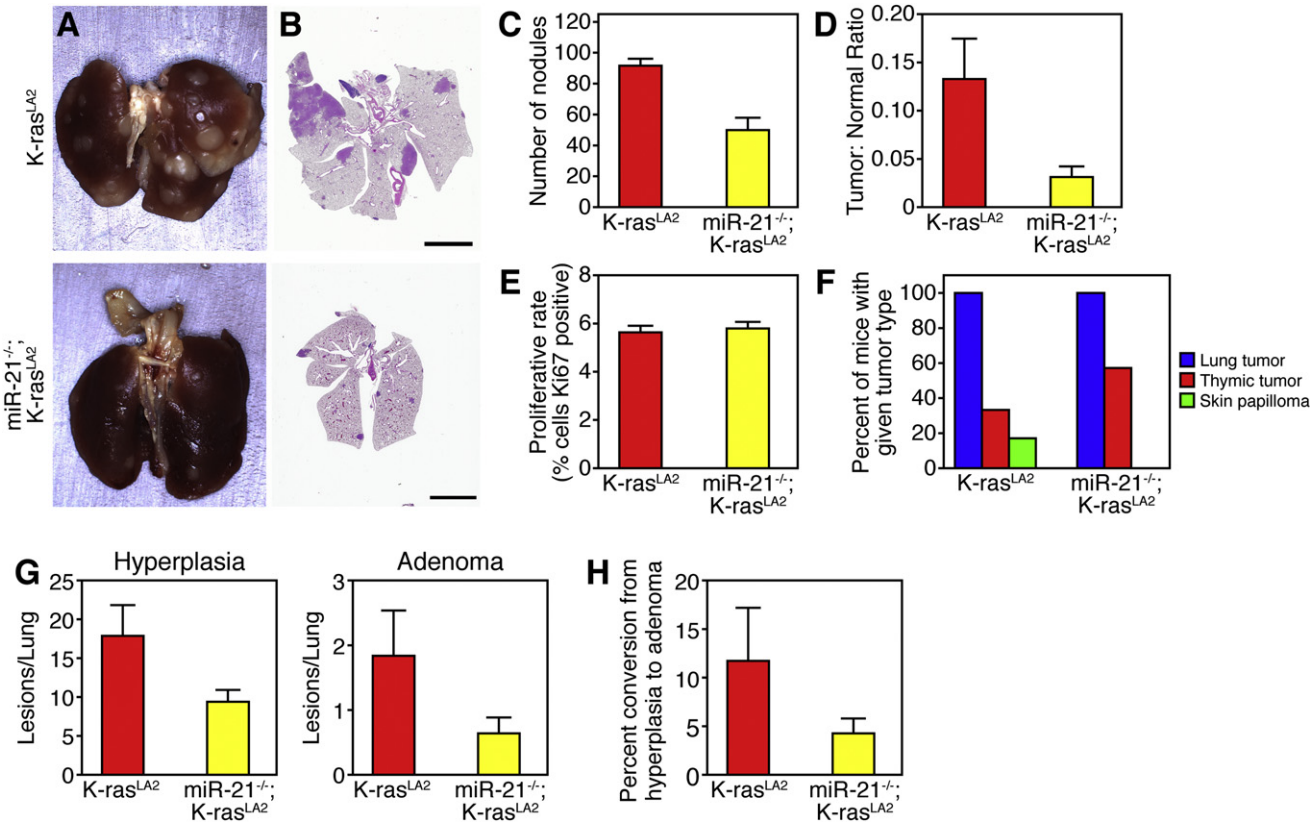

Figure 2. *miR-21* Deletion Suppresses Tumorigenesis in K-ras^{LA2} Model of NSCLC

(A and B) Gross (A) and cross-sectional (B) H&E histology of lungs isolated from *miR-21*$^{-/-}$;*K-ras*^{LA2} and *K-ras*^{LA2} mice at 20 weeks of age. The scale bar represents 5 mm.

(C) Quantification of nodules grossly visible on the lung surface of *miR-21*$^{-/-}$;*K-ras*^{LA2} (n = 5) and *K-ras*^{LA2} (n = 3) mice at 20 weeks of age. Results are mean ± SEM; p = 0.008 using two-tailed, unpaired Student's t test.

(D) Tumor burden measured as the ratio of total tumor area to total lung area of the lungs counted in (C). Results are mean ± SEM; p = 0.015 using two-tailed, unpaired Student's t test.

(E) Quantification of proliferating cells detected by Ki67 antibody immunostaining of lung tumors. Results are mean ± SEM (n = 6); p = 0.4 by two-tailed, unpaired Student's t test.

(F) Tumor spectra in *K-ras*^{LA2} and *miR-21*$^{-/-}$;*K-ras*^{LA2} mice.

(G) Lung H&E cross-sections from *miR-21*$^{-/-}$;*K-ras*^{LA2} (n = 14) mice. *K-ras*^{LA2} (n = 6) mice were analyzed and all lesions were classified for tumor grade. For hyperplasia, p = 0.023. For adenoma, p = 0.057. All data are represented as the mean ± SEM of the number of lesions per lung.

(H) Rate of conversion of hyperplasia to adenoma. Data are presented as mean ± SEM; p = 0.089. See also Figure S2.

miR-21 Targets Multiple Negative Regulators of Ras Signaling

Multiple negative regulators of the Ras/MEK/ERK pathway were shown to be direct miR-21 target genes by luciferase reporter assays (Figure 3B). Although there have been reports of miR-21 target gene regulation in cancer cell lines, the constellation of genes regulated by miR-21 in NSCLC in vivo remains elusive. We hypothesize that increased miR-21 expression potentiates Ras signaling through inhibition of antagonists of the Ras pathway, such as *Spry1*, *Spry2*, *Btg2*, and *Pdcd4* (Casci et al., 1999; Hanafusa et al., 2002; Lo et al., 2006).

We isolated individual tumors from mice, made whole tumor lysates, and performed western blots for putative miR-21 targets to address the effect of miR-21 expression on the protein levels of the miR-21 target genes in vivo within lung tumors. miR-21 overexpression in *CAG-miR-21;K-ras*^{LA2} mutant tumors decreases Spry1, Spry2, and Btg2 protein expression compared to *K-ras*^{LA2} tumors (Figure 4C). The decrease in Spry1, Spry2, and Btg2 in *CAG-miR-21;K-ras*^{LA2} tumors correlates with increased Ras pathway activity, shown by increased ERK phosphorylation (Figure 4C). *miR-21*$^{-/-}$;*K-ras*^{LA2} mutant tumors did not show alteration in the regulation of ERK by Spry1, Spry2, and Btg2 (Figure 4D). Protein analysis of individually isolated tumors showed that Pdcd4 levels were decreased in *CAG-miR-21;K-ras*^{LA2} compound mutant mice compared to *K-ras*^{LA2} control tumors (Figure 4C). This regulation was absent in tumors from the *miR-21*$^{-/-}$;*K-ras*^{LA2} compound mutant mice (Figure 4D). *RECK*, *Cdc25a*, *Map2k3*, *NfiB*, *Trp63*, and *Ski* have been shown to be miR-21 target genes in vitro, but only RECK showed decreased protein levels in the *CAG-miR-21;K-ras*^{LA2} tumors (Figure S3A). Several components of the PI3K pathway, including *PTEN* and *PIK3R1*, have been suggested as miR-21 target genes (Meng et al., 2007); however, miR-21 overexpression did not alter PTEN and PIK3R1 protein expression or Akt

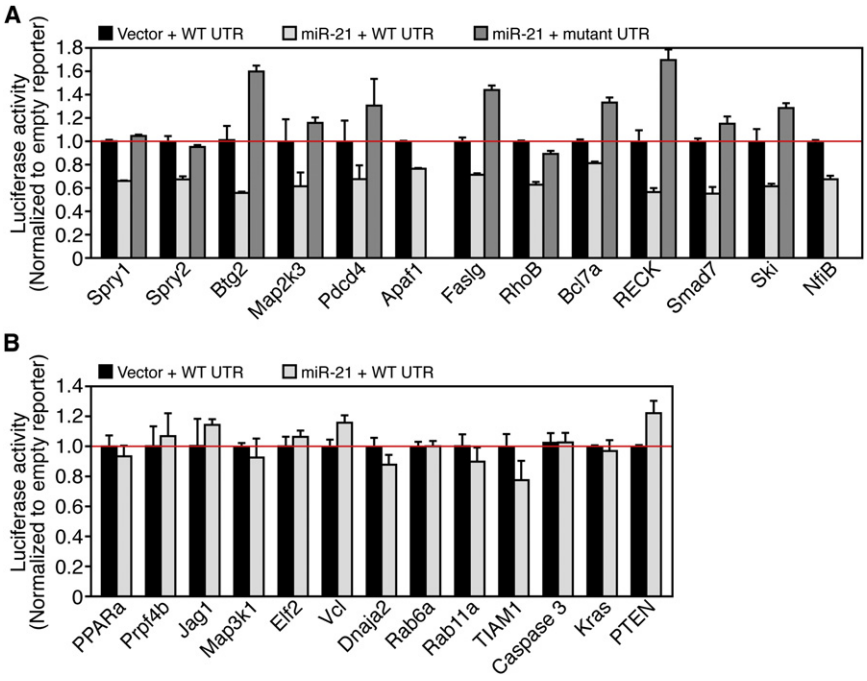

Figure 3. *miR-21* Targets mRNAs Encoding Multiple Tumor Suppressors

(A) Luciferase activity in COS cells cotransfected with miR-21 or control vector and *miR-21*-responsive target gene 3′ UTRs or miR-21 site mutant 3′ UTR luciferase reporters. Data are presented as mean ± SEM and normalized to empty vector (no miR-21) control (n = 4).

(B) Luciferase activity in COS cells cotransfected with miR-21 or empty vector and indicated miR-21 unresponsive 3′ UTRs. Data are presented as mean ± SEM and normalized to empty vector (no miR-21) control (n = 4).

phosphorylation (Figure S3B). These data show that miR-21 overexpression decreases the protein expression of four miR-21 target genes that are tumor suppressors and negative regulators of the Ras/MEK/ERK pathway, resulting in a concomitant increased ERK activity.

miR-21 Suppresses Apoptosis by Targeting Proapoptotic Genes

Next, we evaluated the effect of miR-21 expression on apoptosis. MiR-21 overexpression in *CAG-miR-21;K-ras^{LA2}* mice reduced apoptosis in lung tumors, as shown by TUNEL staining (Figures 5A and 5B). Deletion of miR-21 had no effect on the amount of apoptosis in the lung lesions, as detected by TUNEL, suggesting that lung tumors that develop in the background of the genetic deletion of *miR-21* have escaped miR-21 regulatory effects (Figure 5C). Several miR-21 target genes are tumor suppressors involved in apoptosis, including *Apaf11*, *Pdcd4*, *RhoB*, and *Faslg*. Lysates from individually isolated tumors from *CAG-miR-21;K-ras^{LA2}* mice showed

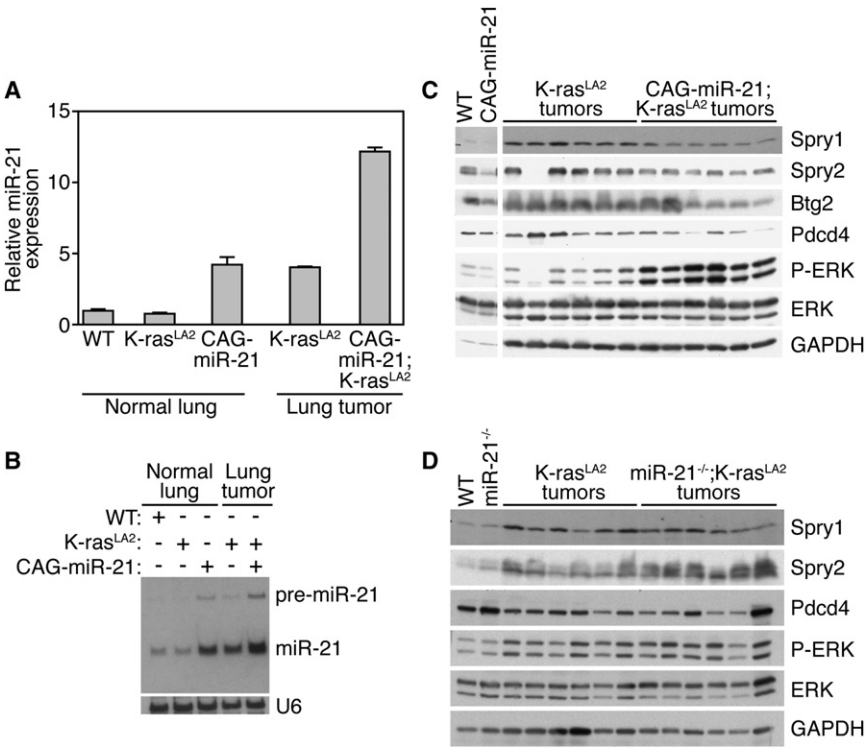

Figure 4. *miR-21* Induction by Oncogenic K-Ras Represses Negative Regulators of the Ras/MEK/ERK Pathway

(A) *MiR-21* expression in lung tumors from *CAG-miR-21;K-ras^{LA2}* and *K-ras^{LA2}* mice (after K-ras activation) compared to normal lung from wild-type (WT), *K-ras^{LA2}* (prior to K-ras activation), and *CAG-miR-21* mice by real-time PCR. Results represent mean ± SEM.

(B) Northern blot analysis of *miR-21* expression in lung tumors from *CAG-miR-21;K-ras^{LA2}* and *K-ras^{LA2}* mice (after K-ras activation) compared to normal lung from WT, *K-ras^{LA2}* (prior to K-ras activation), and *CAG-miR-21* mice.

(C) Western blot analysis of lung lysates from normal lung from WT and *CAG-miR-21* mice and six isolated lung tumors from *CAG-miR-21;K-ras^{LA2}* and *K-ras^{LA2}* mice. Antibodies used are shown on right.

(D) Western blot analysis of lung lysates from WT and *miR-21$^{-/-}$* mice and six isolated tumors from *miR-21$^{-/-}$;K-ras^{LA2}* and *K-ras^{LA2}* mice. Antibodies used are shown on right. See also Figure S3.

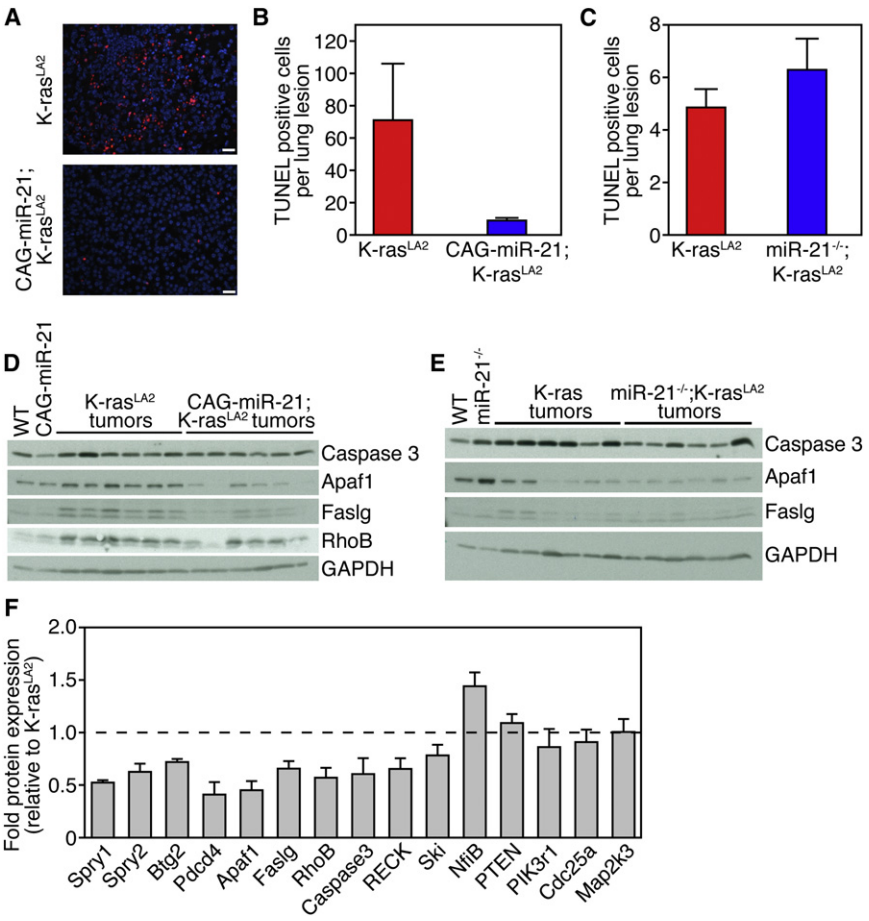

Figure 5. miR-21 Reduces Apoptosis through Targeting Multiple Apoptotic Modulators

(A) TUNEL staining of *K-ras*^{LA2} and *CAG-miR-21; K-ras*^{LA2} tumors. Scale bars represent 20 μm.

(B) Quantification of TUNEL-positive nuclei per lung tumor in *K-ras*^{LA2} (n = 16) and *CAG-miR-21;K-ras*^{LA2} (n = 62) mice. Results are mean ± SEM; p = 0.007 by unpaired, two-tailed Student's t test.

(C) Quantification of TUNEL staining in *miR-21*$^{-/-}$*; K-ras*^{LA2} (n = 22) mice and *K-ras*^{LA2} controls. Results are mean ± SEM; p = 0.28 with unpaired, two-tailed Student's t test.

(D) Western blot analysis of lung lysates from wild-type (WT) and *CAG-miR-21* mice and six isolated lung tumors from *CAG-miR-21;K-ras*^{LA2} and *K-ras*^{LA2} mice. Antibodies used are shown on right.

(E) Western blot analysis of lung lysates from WT and *miR-21*$^{-/-}$ mice and six isolated lung tumors from *miR-21*$^{-/-}$*;K-ras*^{LA2} and *K-ras*^{LA2} mice. Antibodies are shown on right.

(F) Quantification of protein expression from Western blots shown in Figure 4C, Figure 5D, and Figures S3A and S3B. Bar values indicate the mean ± SEM of protein levels in six independent tumors from *CAG-miR-21;K-ras*^{LA2} mice after normalization to GAPDH and represented as fraction of the protein levels in the *K-ras*^{LA2} controls. Dashed line indicates the protein level in *K-ras*^{LA2} tumors.

decreased expression of *Apaf1*, *Caspase 3*, *Pdcd4*, *Faslg*, and *RhoB* (Figures 4C and 5D). *MiR-21*$^{-/-}$*;K-ras*^{LA2} mutant tumors did not show alteration in the regulation of Apaf1 or Faslg (Figure 5E). Apaf1, Pdcd4, Faslg, and RhoB were validated as direct miR-21 target genes by luciferase reporter assays; however, caspase 3 was not directly regulated by miR-21 (Figure 3B). Quantification of miR-21 target Western blots is shown in Figure 5F. These data illustrate that miR-21 overexpression decreases the protein expression of four miR-21 target genes that are involved in apoptosis thus promoting survival.

miR-21 Deletion Sensitizes Cells to DNA-Damaging Chemotherapy

Recent studies illustrate that miRNAs modulate sensitivity of cells to chemotherapy (Blower et al., 2008). We utilized the *miR-21*$^{-/-}$ and wild-type MEFs immortalized with TAg and transformed with RasV12 to test the role of miR-21 in doxorubicin-induced apoptosis. MEFs were cultured with increasing concentrations of doxorubicin, whole cell lysates were isolated, and apoptotic activity was measured by immunoblotting for cleaved caspase 3. MEFs from *miR-21*$^{-/-}$ mice display increased sensitivity to doxorubicin-induced apoptosis measured by protein levels of cleaved caspase 3 (Figure 6A). *miR-21*$^{-/-}$ MEFs were transduced with a lentivirus expressing miR-21 to rescue the miR-21 deficiency (Figure S4). Lentiviral overexpression of miR-21 decreased cleaved caspase 3 levels compared to empty lentiviral transduced *miR-21*$^{-/-}$ MEFs. The increased sensitivity to doxorubicin-induced apoptosis measured by cleaved caspase 3 levels was confirmed by TUNEL (Figure 6C). Therefore, miR-21 plays a significant role in inhibition of apoptosis thus allowing tumor survival.

DISCUSSION

Our results show that miR-21 expression modulates tumor number, incidence, and size in a mouse lung cancer model initiated by oncogenic *K-ras*^{G12D}, consistent with miR-21 functioning as a tumor promoter. miR-21 was not sufficient in our model for tumorigenesis; however, under the control of other tissue-specific promoters, miR-21 could have cancer related phenotypes. miR-21 modulates several components critical to NSCLC pathogenesis through both relieving antagonism of the Ras pathway and reducing apoptotic effectors (Figure 7). Although we show regulation of protein levels of miR-21 target genes with miR-21 overexpression, we do not observe robust changes in protein levels on miR-21 target genes with miR-21 deletion, suggesting that miR-21 may act through additional mechanisms. By targeting antagonists of Ras/MEK/ERK signaling and proapoptotic genes, miR-21 enhances tumor proliferation and survival, two critical components of tumor promotion.

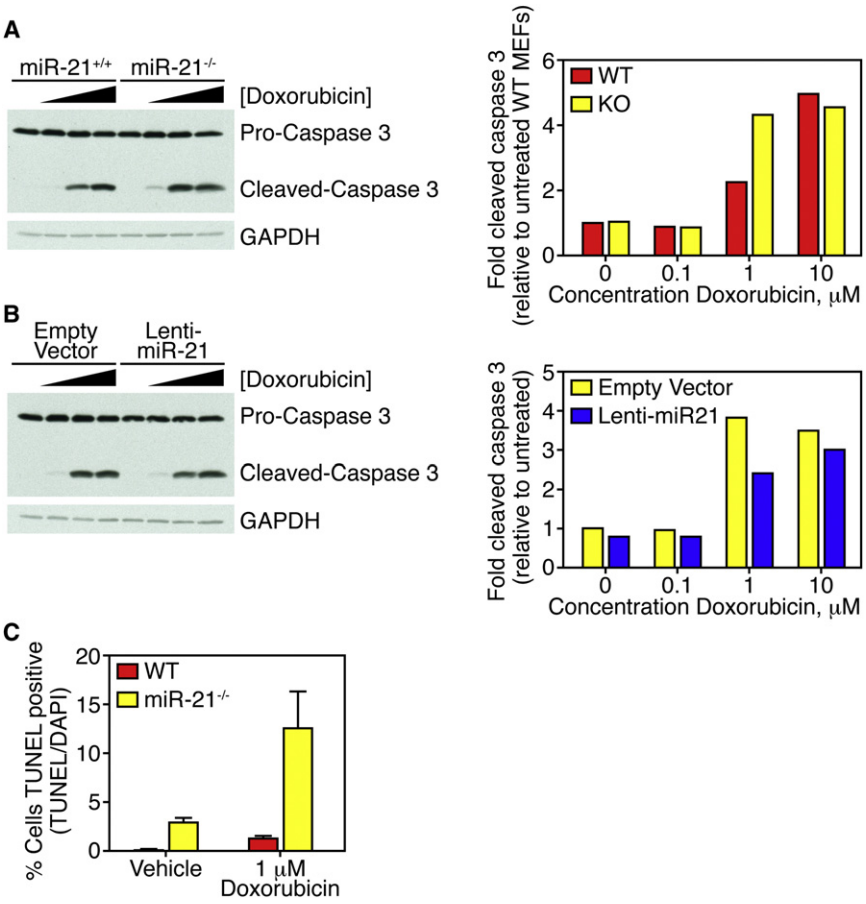

Figure 6. miR-21 Deletion Sensitizes Cells to Doxorubicin-Induced Apoptosis

(A) Western blot analysis (left panel) for cleaved caspase 3 in protein lysates from wild-type and *miR-21*$^{-/-}$ MEFs immortalized with T-Ag, transformed with H-rasV12, and treated with increasing concentrations of doxorubicin. Antibodies used are shown on right. Quantification of cleaved caspase 3 levels normalized to pro-caspase 3 and represented relative to untreated wild-type MEFs (right panel).

(B) Western blot analysis (left panel) for cleaved caspase 3 in protein lysates from *miR-21*$^{-/-}$ MEFs immortalized with T-Ag, transformed with H-rasV12, and transduced with lentivirus expressing miR-21 (lenti-miR-21) or empty vector, and treated with increasing concentrations of doxorubicin. Antibodies used are shown on right. Quantification of cleaved caspase 3 levels normalized to pro-caspase 3 and represented relative to untreated wild-type MEFs (right panel).

(C) TUNEL assay of wild-type and *miR-21*$^{-/-}$ MEFs treated with vehicle or 1 μM doxorubicin for 12 hr. Data are presented as mean ± SEM (n = 6). See also Figure S4.

Our results define in vivo an autoregulatory loop between oncogenic Ras and miR-21 mediated by Spry1, Spry2, Btg2, and Pdcd4. *PDCD4* is a proapoptotic tumor suppressor gene and has been verified as a miR-21 target in human colorectal and breast cancer cell lines (Afonja et al., 2004; Asangani et al., 2008; Bitomsky et al., 2008; Frankel et al., 2008; Lu et al., 2008; Zhang et al., 2006). Pdcd4 functions both as an inducer of apoptosis and a suppressor of AP-1 activity (Hwang et al., 2007).

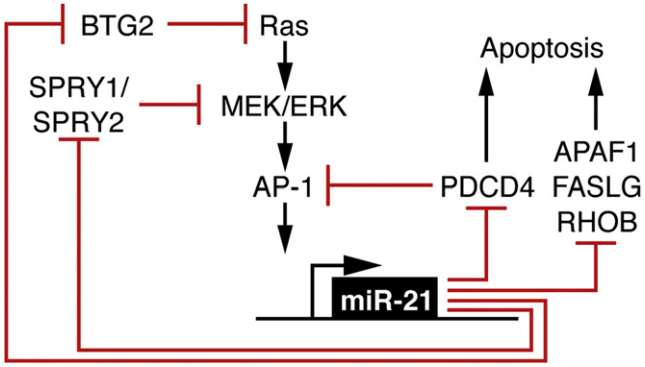

Figure 7. Autoregulatory Loop between Ras and miR-21

Proposed model showing that miR-21 potentiates oncogenic Ras signaling and attenuates apoptosis through repression of multiple tumor suppressors and miR-21 target genes.

Loss of *PDCD4* expression in human lung cancer correlates with higher grade and disease stage (Chen et al., 2003). MiR-21 targets *SPRY2* in cardiomyocytes and SW480 colon cancer cells, enhancing cell migration (Sayed et al., 2008). *SPRY2*, in turn, negatively regulates Ras/MEK/ERK signaling and is a tumor suppressor in NSCLC in both mice (Minowada and Miller, 2004; Minowada and Miller, 2009; Shaw et al., 2007) and humans (Sutterluty et al., 2007). In laryngeal carcinoma, miR-21 targets *BTG2* (Liu et al., 2009), a p53 target gene, recently shown to suppress oncogenic Ras activity by reducing the GTP-bound, active state (Buganim et al., 2010). Although the reductions in protein levels of individual miR-21 targets appear modest with miR-21 overexpression, collectively this diminution of tumor suppressor activity allows for more robust tumor formation through relieving multiple nodes of inhibition of the Ras/MEK/ERK pathway, thus facilitating tumor proliferation.

Oncogenic Ras activation has been shown to increase the expression of Spry2, providing feedback inhibition of Ras activation (Shaw et al., 2007). We show that Ras activation increases miR-21 expression and, in turn, decreases the expression of *Spry2*. The genetic deletion of *miR-21* removes the miR-21 mediated downregulation of Spry2, resulting in more Spry2-mediated Ras/MEK/ERK inhibition and tumor suppressor activity. We postulate that the tumors formed in the background of miR-21 deletion have developed escape mechanisms to circumvent the Spry2 tumor suppressor activity. The necessity to circumvent the lack of miR-21 protumorigenic effects could explain the latency of tumor formation in the *miR-21*$^{-/-}$ mice.

Previous work in cancer cell lines has implicated miR-21 as a suppressor of apoptosis. Knock-down of miR-21 in glioblastoma cell lines triggers the activation of caspases and increases

apoptosis (Chan et al., 2005). Zhang et al. (2008) showed in a human gastric cancer cell line that forced overexpression of miR-21 enhanced tumor proliferation and invasion and knockdown of miR-21 resulted in a marked reduction in proliferation and increase in apoptosis. The present work illustrates in vivo that increased expression of miR-21 significantly reduces apoptosis in mouse lung tumors. MiR-21 overexpression resulted in reduced protein levels of Apaf1, a key component of the intrinsic, mitochondrial apoptotic pathway, as well as decreased expression of Faslg, a key initiator of the extrinsic, death receptor apoptotic pathway. *Faslg* mRNA is expressed in human lung tumors; however, the Faslg protein is only detected in a small fraction of lung tumors (Badillo-Almaraz et al., 2003). miR-21-mediated translational inhibition could partially explain this finding. Overexpression of miR-21 correlated with a decrease RhoB protein levels. RhoB promotes growth inhibition and induces apoptosis in cancer cells (Kim et al., 2009), and *RhoB* expression is downregulated in human NSCLC, suggesting a role as a tumor suppressor gene (Sato et al., 2007). Relieving miR-21 inhibition of proapoptotic genes could provide a means to augment the effect of current chemotherapy.

Methods have been developed to manipulate miRNA function pharmacologically, facilitating the development of new cancer therapeutic strategies (Hutvagner et al., 2004; Krutzfeldt et al., 2005). Increased sensitivity to DNA-damaging agents in the *miR-21*$^{-/-}$-transformed MEFs suggests that inhibition of miR-21 could provide a therapeutic strategy in NSCLC. In addition, inhibiting miR-21 potentially restores the activity of multiple tumor suppressors acting at various critical nodes of tumor development. Here we report an in vivo, functional role of miR-21 in NSCLC.

EXPERIMENTAL PROCEDURES

Mouse Strains

K-ras^{LA2} mice in the B6.129S background were provided by T. Jacks (Massachusetts Institute of Technology) through the National Cancer Institute. Construction of *CAG-Z-miR-21-EGFP* transgenic mice is detailed in Supplemental Experimental Procedures. All mice used in these studies were of mixed genetic backgrounds, and all comparisons were performed on littermate controls. The *CAG-miR-21* transgenic mice (B6C3F1 background) were bred to *K-ras*^{LA2} mice to generate miR-21 overexpressing *CAG-miR-21;K-ras*^{LA2} compound mutant mice and control *K-ras*^{LA2} mice. The *miR-21*$^{-/-}$ mice (B6.129SvEv) were bred to *K-ras*^{LA2} mice to generate *miR-21*-deficient *miR-21*$^{-/-}$*;K-ras*^{LA2} compound mutant mice and control *K-ras*^{LA2} mice. Mice were sacrificed at stated time points or when showing obvious tumor burden or distress, and a full necropsy was performed. All experimental procedures involving animals in this study were reviewed and approved by the Institutional Animal Care and Use Committee at the University of Texas Southwestern Medical Center. For survival analysis, *CAG-miR-21;K-ras*^{LA2} and *K-ras*^{LA2} mice were observed daily from birth and were sacrificed at the first sign of shortness of breath, reduced locomotion, or reduced body weight (>20% of total body weight).

RNA Purification, RT-PCR, and Real-Time PCR

Total RNA was isolated from normal lung or lung tumors with Trizol reagent (Invitrogen) according to the manufacturer's protocol. miRNA levels were determined by Northern blot analysis and real-time PCR. RT-PCR was performed using the TaqMan microRNA reverse-transcriptase kit (Applied Biosystems). Real-time PCR was performed using TaqMan probes on an ABI-PE Prism 7000 sequence detection system according to the manufacturer's protocol. The relative quantities of miRNA were determined using the CT method and were normalized to RNU6B. The recombination of the *K-ras*^{LA2} allele was determined by RT-PCR. Total RNA was isolated from microdissected normal lung and lung tumors. Reverse transcription was performed using random hexamer primers and SuperScript III First-Strand Synthesis (Invitrogen). PCR primers used and conditions were previously described (Johnson et al., 2001).

Northern Blot Analysis

Ten micrograms of total RNA from different tissues or tumors was resolved on a 20% polyacrylamide (7.6 M urea) gel in 1× TBE. RNA was then transferred onto a Zetaprobe GT membrane (Bio-Rad) in 0.5× TBE buffer at 80 V for 1 hr. Hybridization was performed at 39°C. ^{32}P-labeled Star-Fire oligonucleotide probes (IDT) against the mature miR-21 and U6 were used in hybridization. U6 was used as a loading control.

Histology, Immunohistochemistry, and TUNEL

For determining tumor incidence and grade, whole lungs were manually inflated with 10% neutral-buffered formalin, placed in fixative for 3 days, embedded in paraffin, and sectioned at the level of the tracheal bifurcation at 5 μm intervals. H&E stains were performed using standard procedures. Lung and tumor areas were determined using ImageJ software. Tumor burden was expressed as the sum of the tumor area divided by the total lung area. Proliferation was assessed by immunohistochemistry using antibodies against Ki67 (Abcam). Paraffin-embedded sections were deparaffinized, heated in a microwave in 0.01 M sodium citrate buffer for antigen retrieval, treated with 3% H_2O_2 for 10 min, and rinsed in H_2O and PBS. Sections were blocked in 5% goat serum in PBS followed incubation with anti-Ki67 antibody (Abcam). Signals were detected with Vectastain ABC kit (Vector Laboratories) and 3,3′-diaminobenzidine (DAB) substrate (Vector Laboratories). Sections were counterstained with hematoxylin and mounted. Ki67 positive cells were scored per high-power field from three separate animals (four tumors per animal), and each genotype and represented as the mean percentage of the total number of cells ± SEM. Apoptosis was evaluated by staining paraffin sections with In situ cell death detection kit, TMR red terminal deoxynucleotidyl-transferase-mediated dUTP nick-end labeling (TUNEL) system (Roche) according to the manufacturer's protocol. Slides were mounted with Vectashield mounting medium with DAPI (Vector Laboratories). The number of apoptotic cells per lung tumor were recorded and presented as the mean ± SEM.

Tumor Grading

All tumors from the survival cohort were analyzed on H&E sections and categorized as hyperplasia, atypical adenomatous hyperplasia, adenoma, adenoma with typia, and adenocarcinoma, according to the Mouse Models of Human Cancer Consortium recommendations (Nikitin et al., 2004).

Western Blot Analysis

Individual tumors were microdissected from the lungs and snap frozen in liquid nitrogen. Individual tumor and lung lysates were prepared in RIPA with protease inhibitors (Roche complete mini) and phosphatase inhibitor cocktail (Sigma) using a manual pestle homogenizer and clarified by centrifugation at 12,000 *g* for 10 min at 4°C. Protein concentration was determined by BCA assay (Themo Scientific), and equivalent amounts were resolved by SDS-PAGE and immunoblotted by a standard protocol. Antibodies were purchased from Abcam (Spry1, Spry2, Btg2, NfiB, Ski, and Trp63), Cell Signaling (phosphor-ERK, total ERK, total Caspase 3, Apaf1, RhoB, PTEN, PIK3R1, phosphor-Akt(Ser473), total Akt, RECK, Cdc25a, and Map2k3), Chemicon (GAPDH and Faslg), and Rockland (Pdcd4). Quantification of Western blots was performed by densitometry using NIH ImageJ software. Each sample was normalized to GAPDH and represented as a fraction of *K-ras*^{LA2} control tumors.

Reporter Assays

The 466 base-pair genomic fragment encompassing *miR-21* was amplified by PCR and ligated into pCMV6. Full-length 3′ UTRs of putative miR-21 target genes were cloned from mouse 129SvEv genomic DNA and subcloned into the pMiR-report vector (Ambion). Mutations in the putative miR-21 site in the 3′ UTRs were generated by QuickChange mutagenesis (Stratagene) to alter the second and third nucleotides of the targeting sequence. Cell culture, transfection, and luciferase reporter assays were performed as previously described (van Rooij et al., 2008).

Doxorubicin-Induced Apoptosis

Wild-type and *miR-21*$^{-/-}$ MEFs immortalized with T-Ag and transformed with H-ras^{V12} were seeded in a 6-well plate at 1 × 10^5 cells per well. Cells were treated with vehicle control and increasing doxorubicin concentrations from 100 nM to 10 μM for 12 hr. Cells were lysed in RIPA, and protein concentrations were determined by BCA (Thermo Scientific). Western blotting of 50 μg of lysates was performed with antibodies directed against pro- and cleaved Caspase 3 (Cell Signaling) and GAPDH (Chemicon). Quantification of Western blots was performed by densitometry using NIH ImageJ software. Cleaved caspase 3 levels were expressed as a ratio of pro-caspase 3 and were normalized to either WT untreated or empty vector untreated samples. For TUNEL assays, MEFs were seeded in a 6-well plate at 1 × 10^5 cells per well on coverslips. Cells were treated with vehicle control or 1 μM doxorubicin for 12 hr. TUNEL was performed using an in situ cell death detection kit, TMR red terminal deoxynucleotidyl-transferase-mediated dUTP nick-end labeling (TUNEL) system (Roche) according to manufacturer's protocol.

Statistical Analysis

Results are expressed as the mean ± SEM. We utilized a two-tailed, unpaired Student's t test for all pair-wise comparisons (GraphPad Prism version 5). p values less than 0.05 were considered significant.

SUPPLEMENTAL INFORMATION

Supplemental Information includes four figures and Supplemental Experimental Procedures and can be found with this article online at doi:10.1016/j.ccr.2010.08.013.

ACKNOWLEDGMENTS

We are grateful to John McAnally for transgenic injection, Jose Cabrera for figure preparation, and Lillian Sutherland and John Shelton for experimental assistance. Work in Eric Olson's laboratory was supported by grants from the National Institutes of Health, the Leducq Foundation, the Robert A. Welch Foundation (grant number 1-0025), and the American Heart Association: Jon Holden DeHaan Foundation. E.V.R. was supported by grants from the American Heart Association. Mark E. Hatley is a Pediatric Scientist Development Program Fellow sponsored by the Eunice Shriver Kennedy National Institute of Child Health and Human Development (NICHD Grant Award K12-HD000850). E.N.O. and E.V.R. hold equity in miRagen Therapeutics, which is developing miRNA-based therapies for muscle disease.

M.E.H. and E.N.O. developed hypotheses, designed experiments, and wrote the manuscript. M.E.H. and R.B.D. designed animal protocols and experiments. M.E.H. and M.R.G. executed experiments. D.P. and E.V.R. developed and provided the miR-21 knock-out mouse. J.A.R. provided pathological review of histology.

Received: May 10, 2010
Revised: July 6, 2010
Accepted: July 30, 2010
Published: September 13, 2010

REFERENCES

Afonja, O., Juste, D., Das, S., Matsuhashi, S., and Samuels, H.H. (2004). Induction of PDCD4 tumor suppressor gene expression by RAR agonists, antiestrogen and HER-2/neu antagonist in breast cancer cells. Evidence for a role in apoptosis. Oncogene *23*, 8135–8145.

Asangani, I.A., Rasheed, S.A., Nikolova, D.A., Leupold, J.H., Colburn, N.H., Post, S., and Allgayer, H. (2008). MicroRNA-21 (miR-21) post-transcriptionally downregulates tumor suppressor Pdcd4 and stimulates invasion, intravasation and metastasis in colorectal cancer. Oncogene *27*, 2128–2136.

Badillo-Almaraz, I., Badillo-Salas, C., Villalobos, R., Avalos-Diaz, E., and Herrera-Esparza, R. (2003). Defective expression of FasL and Bax in human lung cancer. Clin. Exp. Med. *3*, 106–112.

Baek, D., Villen, J., Shin, C., Camargo, F.D., Gygi, S.P., and Bartel, D.P. (2008). The impact of microRNAs on protein output. Nature *455*, 64–71.

Bartel, D.P. (2004). MicroRNAs: genomics, biogenesis, mechanism, and function. Cell *116*, 281–297.

Bitomsky, N., Wethkamp, N., Marikkannu, R., and Klempnauer, K.H. (2008). siRNA-mediated knockdown of Pdcd4 expression causes upregulation of p21(Waf1/Cip1) expression. Oncogene *27*, 4820–4829.

Blower, P.E., Chung, J.H., Verducci, J.S., Lin, S., Park, J.K., Dai, Z., Liu, C.G., Schmittgen, T.D., Reinhold, W.C., Croce, C.M., et al. (2008). MicroRNAs modulate the chemosensitivity of tumor cells. Mol. Cancer Ther. *7*, 1–9.

Buganim, Y., Solomon, H., Rais, Y., Kistner, D., Nachmany, I., Brait, M., Madar, S., Goldstein, I., Kalo, E., Adam, N., et al. (2010). p53 Regulates the Ras circuit to inhibit the expression of a cancer-related gene signature by various molecular pathways. Cancer Res. *70*, 2274–2284.

Calin, G.A., and Croce, C.M. (2006). MicroRNA signatures in human cancers. Nat. Rev. Cancer *6*, 857–866.

Casci, T., Vinos, J., and Freeman, M. (1999). Sprouty, an intracellular inhibitor of Ras signaling. Cell *96*, 655–665.

Chan, J.A., Krichevsky, A.M., and Kosik, K.S. (2005). MicroRNA-21 is an antiapoptotic factor in human glioblastoma cells. Cancer Res. *65*, 6029–6033.

Chen, Y., Knosel, T., Kristiansen, G., Pietas, A., Garber, M.E., Matsuhashi, S., Ozaki, I., and Petersen, I. (2003). Loss of PDCD4 expression in human lung cancer correlates with tumour progression and prognosis. J. Pathol. *200*, 640–646.

Cho, W.C. (2007). OncomiRs: The discovery and progress of microRNAs in cancers. Mol. Cancer *6*, 60.

Ciafre, S.A., Galardi, S., Mangiola, A., Ferracin, M., Liu, C.G., Sabatino, G., Negrini, M., Maira, G., Croce, C.M., and Farace, M.G. (2005). Extensive modulation of a set of microRNAs in primary glioblastoma. Biochem. Biophys. Res. Commun. *334*, 1351–1358.

Esquela-Kerscher, A., and Slack, F.J. (2006). Oncomirs—microRNAs with a role in cancer. Nat. Rev. Cancer *6*, 259–269.

Frankel, L.B., Christoffersen, N.R., Jacobsen, A., Lindow, M., Krogh, A., and Lund, A.H. (2008). Programmed cell death 4 (PDCD4) is an important functional target of the microRNA miR-21 in breast cancer cells. J. Biol. Chem. *283*, 1026–1033.

Fukuda, T., Mishina, Y., Walker, M.P., and DiAugustine, R.P. (2005). Conditional transgenic system for mouse aurora a kinase: Degradation by the ubiquitin proteasome pathway controls the level of the transgenic protein. Mol. Cell. Biol. *25*, 5270–5281.

Goke, R., Barth, P., Schmidt, A., Samans, B., and Lankat-Buttgereit, B. (2004). Programmed cell death protein 4 suppresses CDK1/cdc2 via induction of p21 (Waf1/Cip1). Am. J. Physiol. Cell Physiol. *287*, C1541–C1546.

Grimson, A., Farh, K.K., Johnston, W.K., Garrett-Engele, P., Lim, L.P., and Bartel, D.P. (2007). MicroRNA targeting specificity in mammals: Determinants beyond seed pairing. Mol. Cell *27*, 91–105.

Hanafusa, H., Torii, S., Yasunaga, T., and Nishida, E. (2002). Sprouty1 and Sprouty2 provide a control mechanism for the Ras/MAPK signalling pathway. Nat. Cell Biol. *4*, 850–858.

Huang, T.H., Wu, F., Loeb, G.B., Hsu, R., Heidersbach, A., Brincat, A., Horiuchi, D., Lebbink, R.J., Mo, Y.Y., Goga, A., and McManus, M.T. (2009). Up-regulation of miR-21 by HER2/neu signaling promotes cell invasion. J. Biol. Chem. *284*, 18515–18524.

Hutvagner, G., Simard, M.J., Mello, C.C., and Zamore, P.D. (2004). Sequence-specific inhibition of small RNA function. PLoS Biol. *2*, E98.

Hwang, S.K., Jin, H., Kwon, J.T., Chang, S.H., Kim, T.H., Cho, C.S., Lee, K.H., Young, M.R., Colburn, N.H., Beck, G.R., Jr., et al. (2007). Aerosol-delivered programmed cell death 4 enhanced apoptosis, controlled cell cycle and suppressed AP-1 activity in the lungs of AP-1 luciferase reporter mice. Gene Ther. *14*, 1353–1361.

Iorio, M.V., Visone, R., Di Leva, G., Donati, V., Petrocca, F., Casalini, P., Taccioli, C., Volinia, S., Liu, C.G., Alder, H., et al. (2007). MicroRNA signatures in human ovarian cancer. Cancer Res. *67*, 8699–8707.

Jansen, A.P., Camalier, C.E., and Colburn, N.H. (2005). Epidermal expression of the translation inhibitor programmed cell death 4 suppresses tumorigenesis. Cancer Res. *65*, 6034–6041.

Johnson, L., Mercer, K., Greenbaum, D., Bronson, R.T., Crowley, D., Tuveson, D.A., and Jacks, T. (2001). Somatic activation of the K-ras oncogene causes early onset lung cancer in mice. Nature *410*, 1111–1116.

Kim, D.M., Chung, K.S., Choi, S.J., Jung, Y.J., Park, S.K., Han, G.H., Ha, J.S., Song, K.B., Choi, N.S., Kim, H.M., et al. (2009). RhoB induces apoptosis via direct interaction with TNFAIP1 in HeLa cells. Int. J. Cancer *125*, 2520–2527.

Kota, J., Chivukula, R.R., O'Donnell, K.A., Wentzel, E.A., Montgomery, C.L., Hwang, H.W., Chang, T.C., Vivekanandan, P., Torbenson, M., Clark, K.R., et al. (2009). Therapeutic microRNA delivery suppresses tumorigenesis in a murine liver cancer model. Cell *137*, 1005–1017.

Krek, A., Grun, D., Poy, M.N., Wolf, R., Rosenberg, L., Epstein, E.J., MacMenamin, P., da Piedade, I., Gunsalus, K.C., Stoffel, M., and Rajewsky, N. (2005). Combinatorial microRNA target predictions. Nat. Genet. *37*, 495–500.

Krutzfeldt, J., Rajewsky, N., Braich, R., Rajeev, K.G., Tuschl, T., Manoharan, M., and Stoffel, M. (2005). Silencing of microRNAs in vivo with 'antagomirs'. Nature *438*, 685–689.

Lawrie, C.H., Soneji, S., Marafioti, T., Cooper, C.D., Palazzo, S., Paterson, J.C., Cattan, H., Enver, T., Mager, R., Boultwood, J., et al. (2007). MicroRNA expression distinguishes between germinal center B cell-like and activated B cell-like subtypes of diffuse large B cell lymphoma. Int. J. Cancer *121*, 1156–1161.

Lewis, B.P., Burge, C.B., and Bartel, D.P. (2005). Conserved seed pairing, often flanked by adenosines, indicates that thousands of human genes are microRNA targets. Cell *120*, 15–20.

Liu, M., Wu, H., Liu, T., Li, Y., Wang, F., Wan, H., Li, X., and Tang, H. (2009). Regulation of the cell cycle gene, BTG2, by miR-21 in human laryngeal carcinoma. Cell Res. *19*, 828–837.

Lo, T.L., Fong, C.W., Yusoff, P., McKie, A.B., Chua, M.S., Leung, H.Y., and Guy, G.R. (2006). Sprouty and cancer: The first terms report. Cancer Lett. *242*, 141–150.

Lu, Z., Liu, M., Stribinskis, V., Klinge, C.M., Ramos, K.S., Colburn, N.H., and Li, Y. (2008). MicroRNA-21 promotes cell transformation by targeting the programmed cell death 4 gene. Oncogene *27*, 4373–4379.

Lui, W.O., Pourmand, N., Patterson, B.K., and Fire, A. (2007). Patterns of known and novel small RNAs in human cervical cancer. Cancer Res. *67*, 6031–6043.

Ma, L., Young, J., Prabhala, H., Pan, E., Mestdagh, P., Muth, D., Teruya-Feldstein, J., Reinhardt, F., Onder, T.T., Valastyan, S., et al. (2010). miR-9, a MYC/MYCN-activated microRNA, regulates E-cadherin and cancer metastasis. Nat. Cell Biol. *12*, 247–256.

Markou, A., Tsaroucha, E.G., Kaklamanis, L., Fotinou, M., Georgoulias, V., and Lianidou, E.S. (2008). Prognostic value of mature MicroRNA-21 and MicroRNA-205 overexpression in non-small cell lung cancer by quantitative real-time RT-PCR. Clin. Chem. *54*, 1696–1704.

Meng, F., Henson, R., Wehbe-Janek, H., Ghoshal, K., Jacob, S.T., and Patel, T. (2007). MicroRNA-21 regulates expression of the PTEN tumor suppressor gene in human hepatocellular cancer. Gastroenterology *133*, 647–658.

Minowada, G., and Miller, Y.E. (2004). Sprouty 2 gene in mouse lung tumorigenesis. Chest *125* (5 Suppl), 111S.

Minowada, G., and Miller, Y.E. (2009). Overexpression of Sprouty 2 in mouse lung epithelium inhibits urethane-induced tumorigenesis. Am. J. Respir. Cell Mol. Biol. *40*, 31–37.

Nikitin, A.Y., Alcaraz, A., Anver, M.R., Bronson, R.T., Cardiff, R.D., Dixon, D., Fraire, A.E., Gabrielson, E.W., Gunning, W.T., Haines, D.C., et al. (2004). Classification of proliferative pulmonary lesions of the mouse: Recommendations of the mouse models of human cancers consortium. Cancer Res. *64*, 2307–2316.

Parkin, D.M., Bray, F.I., and Devesa, S.S. (2001). Cancer burden in the year 2000: The global picture. Eur. J. Cancer *37* (*Suppl 8*), S4–S66.

Ramalingam, S., Pawlish, K., Gadgeel, S., Demers, R., and Kalemkerian, G.P. (1998). Lung cancer in young patients: analysis of a Surveillance, Epidemiology, and End Results database. J. Clin. Oncol. *16*, 651–657.

Sato, N., Fukui, T., Taniguchi, T., Yokoyama, T., Kondo, M., Nagasaka, T., Goto, Y., Gao, W., Ueda, Y., Yokoi, K., et al. (2007). RhoB is frequently down-regulated in non-small-cell lung cancer and resides in the 2p24 homozygous deletion region of a lung cancer cell line. Int. J. Cancer *120*, 543–551.

Sayed, D., Rane, S., Lypowy, J., He, M., Chen, I.Y., Vashistha, H., Yan, L., Malhotra, A., Vatner, D., and Abdellatif, M. (2008). MicroRNA-21 targets Sprouty2 and promotes cellular outgrowths. Mol. Biol. Cell *19*, 3272–3282.

Seike, M., Goto, A., Okano, T., Bowman, E.D., Schetter, A.J., Horikawa, I., Mathe, E.A., Jen, J., Yang, P., Sugimura, H., et al. (2009). MiR-21 is an EGFR-regulated anti-apoptotic factor in lung cancer in never-smokers. Proc. Natl. Acad. Sci. USA *106*, 12085–12090.

Selbach, M., Schwanhausser, B., Thierfelder, N., Fang, Z., Khanin, R., and Rajewsky, N. (2008). Widespread changes in protein synthesis induced by microRNAs. Nature *455*, 58–63.

Selcuklu, S.D., Donoghue, M.T., and Spillane, C. (2009). miR-21 as a key regulator of oncogenic processes. Biochem. Soc. Trans. *37*, 918–925.

Shaw, A.T., Meissner, A., Dowdle, J.A., Crowley, D., Magendantz, M., Ouyang, C., Parisi, T., Rajagopal, J., Blank, L.J., Bronson, R.T., et al. (2007). Sprouty-2 regulates oncogenic K-ras in lung development and tumorigenesis. Genes Dev. *21*, 694–707.

Si, M.L., Zhu, S., Wu, H., Lu, Z., Wu, F., and Mo, Y.Y. (2007). miR-21-mediated tumor growth. Oncogene *26*, 2799–2803.

Soon, Y.Y., Stockler, M.R., Askie, L.M., and Boyer, M.J. (2009). Duration of chemotherapy for advanced non-small-cell lung cancer: A systematic review and meta-analysis of randomized trials. J. Clin. Oncol. *27*, 3277–3283.

Subramanian, S., Lui, W.O., Lee, C.H., Espinosa, I., Nielsen, T.O., Heinrich, M.C., Corless, C.L., Fire, A.Z., and van de Rijn, M. (2008). MicroRNA expression signature of human sarcomas. Oncogene *27*, 2015–2026.

Sutterluty, H., Mayer, C.E., Setinek, U., Attems, J., Ovtcharov, S., Mikula, M., Mikulits, W., Micksche, M., and Berger, W. (2007). Down-regulation of Sprouty2 in non-small cell lung cancer contributes to tumor malignancy via extracellular signal-regulated kinase pathway-dependent and -independent mechanisms. Mol. Cancer Res. *5*, 509–520.

Talotta, F., Cimmino, A., Matarazzo, M.R., Casalino, L., De Vita, G., D'Esposito, M., Di Lauro, R., and Verde, P. (2009). An autoregulatory loop mediated by miR-21 and PDCD4 controls the AP-1 activity in RAS transformation. Oncogene *28*, 73–84.

Tran, N., McLean, T., Zhang, X., Zhao, C.J., Thomson, J.M., O'Brien, C., and Rose, B. (2007). MicroRNA expression profiles in head and neck cancer cell lines. Biochem. Biophys. Res. Commun. *358*, 12–17.

van Rooij, E., Sutherland, L.B., Liu, N., Williams, A.H., McAnally, J., Gerard, R.D., Richardson, J.A., and Olson, E.N. (2006). A signature pattern of stress-responsive microRNAs that can evoke cardiac hypertrophy and heart failure. Proc. Natl. Acad. Sci. USA *103*, 18255–18260.

van Rooij, E., Sutherland, L.B., Thatcher, J.E., DiMaio, J.M., Naseem, R.H., Marshall, W.S., Hill, J.A., and Olson, E.N. (2008). Dysregulation of microRNAs after myocardial infarction reveals a role of miR-29 in cardiac fibrosis. Proc. Natl. Acad. Sci. USA *105*, 13027–13032.

Ventura, A., and Jacks, T. (2009). MicroRNAs and cancer: Short RNAs go a long way. Cell *136*, 586–591.

Volinia, S., Calin, G.A., Liu, C.G., Ambs, S., Cimmino, A., Petrocca, F., Visone, R., Iorio, M., Roldo, C., Ferracin, M., et al. (2006). A microRNA expression signature of human solid tumors defines cancer gene targets. Proc. Natl. Acad. Sci. USA *103*, 2257–2261.

Voorhoeve, P.M., and Agami, R. (2007). Classifying microRNAs in cancer: The good, the bad and the ugly. Biochim. Biophys. Acta *1775*, 274–282.

Wang, P., Zou, F., Zhang, X., Li, H., Dulak, A., Tomko, R.J., Jr., Lazo, J.S., Wang, Z., Zhang, L., and Yu, J. (2009). microRNA-21 negatively regulates Cdc25A and cell cycle progression in colon cancer cells. Cancer Res. *69*, 8157–8165.

Xie, Y., Todd, N.W., Liu, Z., Zhan, M., Fang, H., Peng, H., Alattar, M., Deepak, J., Stass, S.A., and Jiang, F. (2010). Altered miRNA expression in sputum for diagnosis of non-small cell lung cancer. Lung Cancer *67*, 170–176.

Yanaihara, N., Caplen, N., Bowman, E., Seike, M., Kumamoto, K., Yi, M., Stephens, R.M., Okamoto, A., Yokota, J., Tanaka, T., et al. (2006). Unique

microRNA molecular profiles in lung cancer diagnosis and prognosis. Cancer Cell *9*, 189–198.

Yang, H.S., Jansen, A.P., Komar, A.A., Zheng, X., Merrick, W.C., Costes, S., Lockett, S.J., Sonenberg, N., and Colburn, N.H. (2003). The transformation suppressor Pdcd4 is a novel eukaryotic translation initiation factor 4A binding protein that inhibits translation. Mol. Cell. Biol. *23*, 26–37.

Yang, H.S., Jansen, A.P., Nair, R., Shibahara, K., Verma, A.K., Cmarik, J.L., and Colburn, N.H. (2001). A novel transformation suppressor, Pdcd4, inhibits AP-1 transactivation but not NF-kappaB or ODC transactivation. Oncogene *20*, 669–676.

Zhang, H., Ozaki, I., Mizuta, T., Hamajima, H., Yasutake, T., Eguchi, Y., Ideguchi, H., Yamamoto, K., and Matsuhashi, S. (2006). Involvement of programmed cell death 4 in transforming growth factor-beta1-induced apoptosis in human hepatocellular carcinoma. Oncogene *25*, 6101–6112.

Zhang, Z., Li, Z., Gao, C., Chen, P., Chen, J., Liu, W., Xiao, S., and Lu, H. (2008). miR-21 plays a pivotal role in gastric cancer pathogenesis and progression. Lab. Invest. *88*, 1358–1366.

Zhu, S., Wu, H., Wu, F., Nie, D., Sheng, S., and Mo, Y.Y. (2008). MicroRNA-21 targets tumor suppressor genes in invasion and metastasis. Cell Res. *18*, 350–359.